The impact of environmental and human factors on urban heat and microclimate variability

Authors

Wong Paulina[1], Lai Poh-Chin[1*], Low Chien-Tat[1], Chen Si[1], Hart Melissa[2]

[1] Department of Geography, The University of Hong Kong, Pokfulam Road, Pokfulam, Hong Kong.

[2] Australian Research Council Centre of Excellence for Climate System Science, Climate Change Research Centre. The University of New South Wales, Sydney, Australia; formerly at the Department of Geography, The University of Hong Kong.

Corresponding Author

* Lai Poh-Chin

Department of Geography, The University of Hong Kong, Pokfulam Road, Pokfulam, Hong Kong.

Tel: (852) 3917-2830

Fax: (852) 2559-8994

Email: pclai@hku.hk

Abstract

Urbanization is known to cause noticeable changes in the properties of local climate. Studies have shown that urban areas, compared to rural areas with less artificial surfaces, register higher local temperatures as a result of Urban Heat Islands (UHIs). Hong Kong is one of the most densely populated cities in the world and a high proportion of its population residing in densely built high-rise buildings are experiencing some degrees of thermal discomfort. This study selected Mong Kok and Causeway Bay, two typical urban communities in Hong Kong, to gather evidence of microclimate variation and sources of thermal discomfort. UHIs were estimated from 58 logging sensors placed at strategic locations to take temperature and humidity measurements over 17 consecutive days each in the summer/hot and winter/cool periods. By employing geographic information and global positioning systems, these measurements were geocoded and plotted over the built landscape to convey microclimate variation. The empirical data were further aligned with distinct environmental settings to associate possible factors contributing to UHIs. This study established the existence and extent of microclimate variation of UHI within urban communities of different environmental configuration and functional uses. The findings provided essential groundwork for further studies of UHI effects to inform sources of local thermal discomfort and better planning design to safeguard environmental health in public areas.

Keywords: Microclimate, UHI, thermal comfort, GIS

1. Introduction

The world has undergone rapid industrialization and urbanization in recent centuries. Rapid urban development modifies the natural surface and turns it into manmade structures and built landscapes. These changes have been known to raise local temperatures in urban areas and contribute to the formation of urban heat islands (UHIs). UHIs increase the risks of climatic and biophysical hazards in the urban environment, including heat stress and heightened exposure to air pollutants [1, 2]. At the same time, an increased usage of air conditioning and refrigeration in hotter/humid summers incurs a corresponding increase in the energy consumption with negative impacts on the energy resources of a city [3].

Past UHI-related studies have focused primarily on North American and European countries located in the mid-latitudes. Less than 20 percent of these UHI-related studies was carried out in cities of subtropical climate [4]. Singh [5] estimated that 16 of the world's 24 megacities will be in Asia by 2015. These cities in tropical and subtropical regions have characteristically hot and humid summers with relatively weak winds and occasionally extreme continental climates [4]. The fairly stable and mild climates seemed to favor the rapid growth of population and urbanization [6], further exacerbating the heat island effect. Although UHI is about urban-rural differences, a large variation in climate from region to region makes it difficult to draw generalizations about UHI effects and quantify climate-sensitive urban design guidelines governing street dimensions and orientations for use by urban designers.

Microclimate UHI refers to the climate and UHI intensities of a small community or a cluster of developed areas. It is widely known that each city has its own local scale or microclimate that is uniquely different from regional and global climate patterns. Microclimates are influenced by topography, urban forms, and the presence of water bodies and vegetation [7, 8, 9]. The microclimate scale can be at the levels of community or neighborhood, building block, garden, and even down to the spacing between buildings, such as a street canyon [10, 11]. Although more attention has been made in recent years on examining UHI effects at the microclimate level, the environmental performance of various causative UHI factors in an urban community has remained uncertain [12, 13]. Much of the established microclimate results to date were based on simulated results conducted in wind tunnel facilities and through simulation by computational fluid dynamics [14, 15]. Therefore, urban climate-related studies providing empirical evidence to quantify microclimate UHI effects is vital to understanding the impact of human activities and urban development on longer-term temperature change.

This study is an attempt to patch research gaps in microclimate UHI studies. It demonstrated the feasibility of low-cost sensors in undertaking continuous temperature measurements in a subtropical setting where UHI-related studies have been found inadequate. The integrative use of geographic information systems (GIS) technology in microclimate UHI studies also facilitated temporal and spatial examination of the UHI phenomenon. In addition, our study found key differences in the local environment (vis-à-vis urban morphological features and human activities) that collectively shape the microclimate. It showed that microclimate UHI is strongly affected by the existence of buildings and street canyon geometry amidst other meteorological factors and human activity patterns. The knowledge is essential to derive some parameters governing urban heat fluxes. The method of combining logging sensors and a GIS means that the UHI problem of a community can be examined spatially and effectively at little cost to result in better appreciation of subtle differences in the conditions prevailing over a given landscape. This knowledge can be incorporated into urban planning and design practice to maintain temperatures at a more pleasant level for human thermal comfort and less damaging to human health.

2. Data and Method

The study involved the deployment of multiple temperature sensors in two different urban communities of Hong Kong for internal consistency checks. To enable a structured understanding of microclimate differences, these sensors were mounted in locations with characteristically different environmental settings, including (1) areas traversed by a main road with heavy traffic; (2) areas bordering a secondary road with moderate traffic; (3) areas typified with heavy human activities; (4) open or park areas with greenery; and (5) semi-enclosed areas or tunnels.

2.1 Study Area

Hong Kong, situated along the south east coast of China near the entrance of China's Pearl River Delta (22°15' N, 114°10' E), has an average attitude of 8m above sea level. It is one of the most densely populated cities in the world with a high proportion of its 7 million people concentrating in 265 square kilometers of urban areas or 24 percent of the total land area (1108 square kilometers) [16]. The morphology of Hong Kong is a combination of mountainous terrain and widely scattered urban development with densely built high rises. The climate is a monsoon-influenced humid subtropical climate with hot and humid summers and mild winters according to the Köppen classification Cwa system [17]. Most summer days have characteristically high humidity with warm air coming from the southwest, creating zones of local thermal discomfort.

Mong Kok (MK) is located within the center of the Kowloon Peninsula and Causeway Bay (CWB) along the northern part of Hong Kong Island (Figure 1). Both communities are densely populated and have mixed commercial and residential land uses [18]. They could both be classified as Compact High-Rise Zone (BCZ1) based on the local climate zone (LCZ) defined by Stewart and Oke [19]. MK is situated inland and away from the waterfront with pockets of green areas whereas Causeway Bay is bordering the Victoria Harbor and has a large urban park measuring over 19 hectares [20]. According to a shopping survey conducted by the Hong Kong Planning Department [21], MK and CWB were respectively the first and second most popular shopping districts in Hong Kong as they were characterized by an interesting mix of street markets, street-side retail shops and food stalls, as well as medium- to large- scale shopping malls. They are believed to be two of the most representative urbanized areas with a high level of human activity that require an in-depth analysis of the effects of urbanization on microclimate.

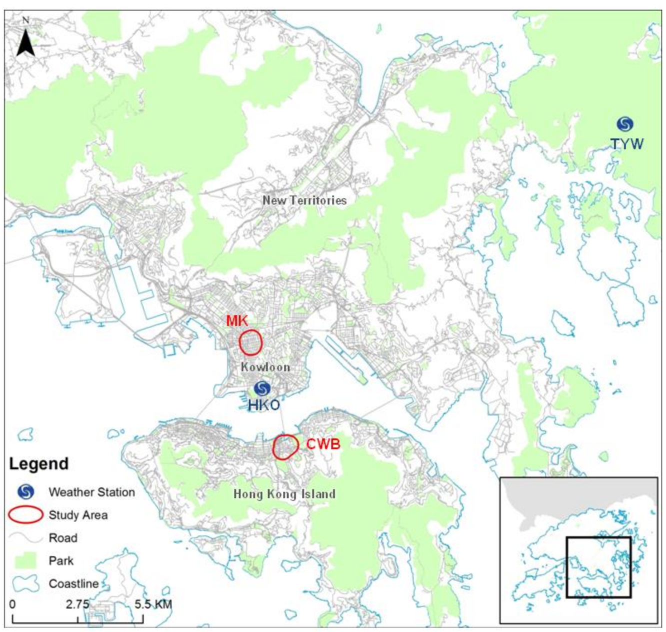

Figure 1: A map of Hong Kong showing locations of Mong Kok (MK) and Causeway Bay (CWB). The Hong Kong Observatory (HKO) and Tsak Yue Wu (TYW) are the designated urban and rural weather stations respectively.

The Mass Transit Railway (MTR)[1] is the most comprehensive transportation system in Hong Kong linking local districts and its exits are known to be core centers with high human activity. Due to ambiguity in identifying geographic boundaries for MK and CWB, radial buffers of 200m and 400m [22, 23] were applied around all MTR exits at each site to embrace its activity areas (Figure 2). Within the buffered areas, the urban morphologies of MK and CWB were characterized by rigid street networks interlaced with built structures. Both communities are facing a large number of urban issues of varying degrees, including crowded settlement, heavy traffic, infrastructure degradation, unfriendly pedestrian environment, and a lack of open space and urban greening (especially in the case of MK).

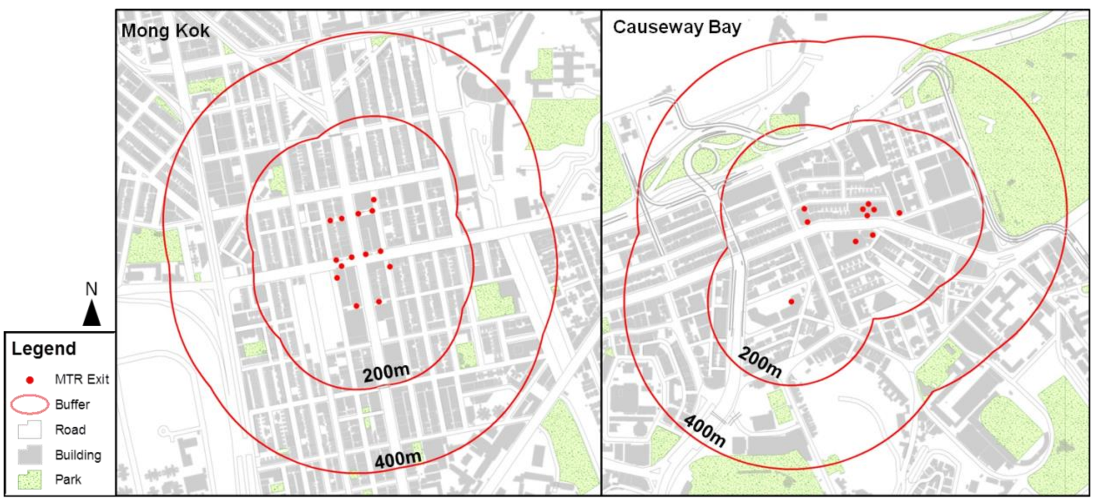

Figure 2: Mong Kok and Causeway Bay with radial buffers of 200m and 400m based on MTR exits.

Figure 2 shows the extent of the study areas in which the 200m buffer zones delimit areas with a concentration of pedestrian flow, as well as commercial and retail activities. The peripheral zones from 200m to 400m represent areas with limited commercial activity to serve planned residential, convenience retail, recreational and other uses. These study areas outline the areal extent to mount temperature sensors to cover locations with the five characteristically different environmental settings explained earlier.

2.2 Instrument and Data Collection

Past research has shown that traffic emission and roadside activities are significant contributors to urban heat [24, 25]. In accordance with standards set by the World Meteorological Organization [26], most of the official weather stations managed by the Hong Kong Observatory (HKO) are situated in park-like settings away from urban streets. This constraint, coupled with a sparse coverage of 43 automatic weather stations for the whole of Hong Kong [27], has prevented detailed examination of UHI in urban communities with well-developed road networks.

A total of 58 small and low-cost Thermochron iButton sensors (DS1923; Maxim/Dallas Semiconductor Corp., USA) [28] were each housed within a non-aspirated solar radiation shield (HOBO Onset RS-3) and mounted on a road-side street sign post with a hose clamp at 2.3 meters above ground (Figure 3) as stipulated by the Highways Department. The sensors took air temperature and relative humidity measurements at every 15-minute interval for 17 consecutive days in the summer (15 September to 1 October 2012) and repeated again in the winter (18 January to 3 February 2013). The weather during these two periods of measurement was clear and calm with mean temperature readings ranging between 26 and 28.5 ºC in the summer and 14.6 and 21.4 ºC in the winter [27].

(a) An iButton housed in a solar radiation shield.

(b) A shielded iButton secured on a street sign post by a stainless steel hose clamp.

Figure 3: Set up of a monitoring sensor.

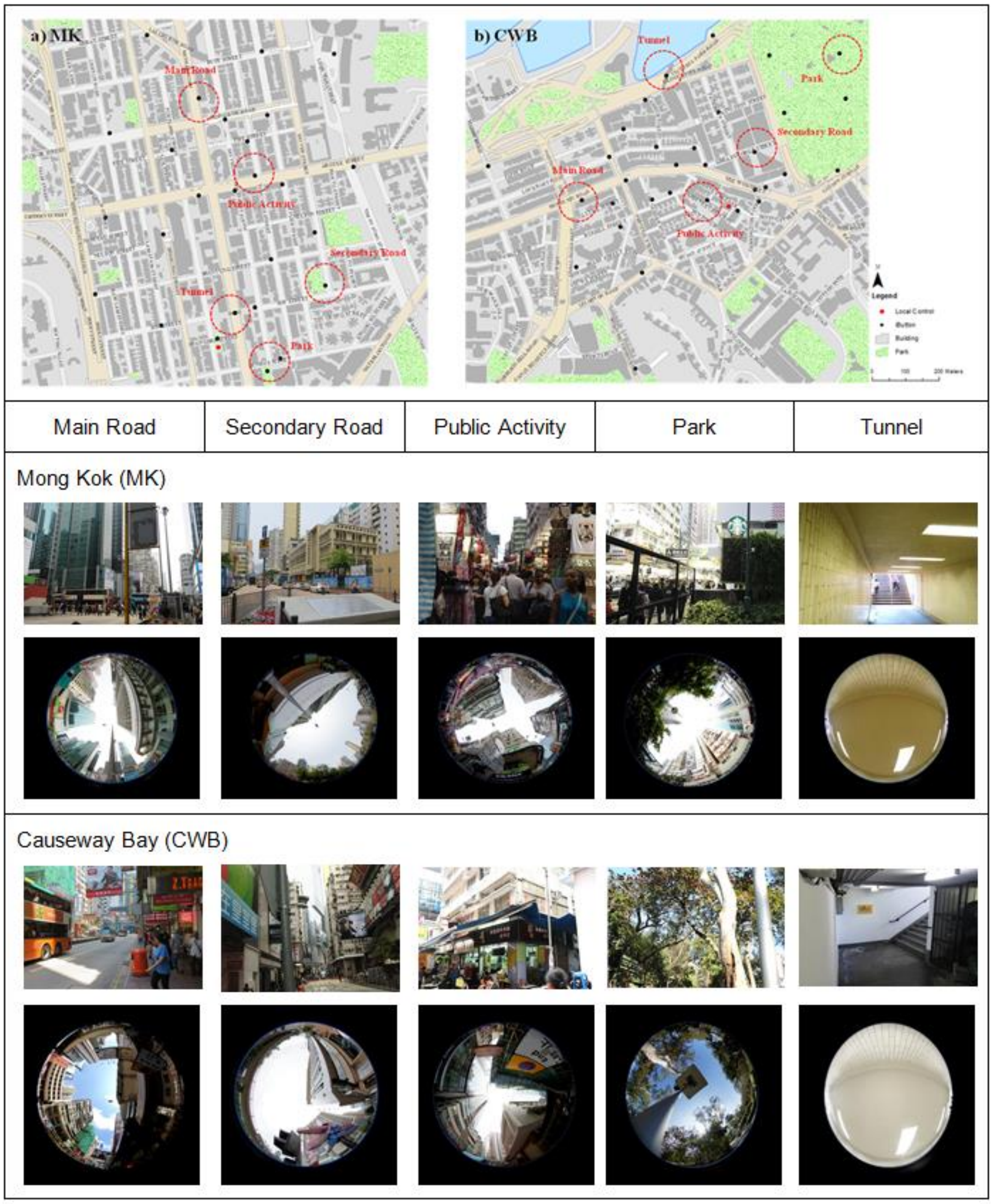

Figure 4: The maps show locations of sensors and local controls in (a) Mong Kok and (b) Causeway Bay. Five different environmental settings were surveyed: main road, secondary road, public activity, park and tunnel. Figure shows photographs of street scenes (first row) and corresponding fisheye images (second row) at the respective survey sites in Mong Kok and Causeway Bay.

The survey locations (26 in MK and 32 in CWB) were decided strategically to include public transit access points (e.g., exits of the MTR stations and bus stops) and locations categorized into five different environmental settings: main road, secondary road, public activity area, park and tunnel (Figure 4). Photographs and fisheye images of the study sites in Figure 4 show dissimilar locational characteristics. The main road setting has wide streets with traffic and surrounded by tall skyscrapers that limit the sky view at street level, as reflected through the fisheye images. The secondary road setting is somewhat similar but with narrower streets and shorter buildings that open the sky view a bit more. Public activity areas are found in narrow streets enclosed by tall buildings to yield limited sky view. Park areas are more open and surrounded by buildings and vegetation, also projected on the fisheye images. Finally, the tunnel setting is a semi-enclosed spaced with no sky view.

Secondary meteorological data were obtained for the designated urban (Hong Kong Observatory - HKO) and rural (Tsak Yue Wu - TYW) weather stations, as a means to cross-validate roadside measurements and also to estimate the UHI effects. The HKO weather station is situated within an urban park in Tsim Sha Tsui, a leading commercial and shopping district in Hong Kong. Although a recognized urban weather station, the HKO has been criticized to underestimate urban temperatures in areas with high human activity [17]. The TYW weather station is situated in rural Sai Kung to the east of Hong Kong. It has been suggested to be a more representative rural station than the one in Ta Kwu Ling whose measurements are likely affected by the nearby financial and trading center of Shenzhen in China [17, 29]. Full meteorological profiles during the measurement period were acquired from the HKO at one-minute interval. Other geospatial GIS data were also acquired from government sources (including Lands, Planning, and Transport Departments) to provide base map, land-use, and traffic information needed for spatial analysis.

2.3 Methods of Analysis

All iButton sensors were calibrated utilizing ice and warm water baths to assure measurement accuracy to well within ±1 °C. Measurements from the sensors were validated against the official urban temperature record at the HKO. The validated measurements collected at study sites were used to compute UHI values [4, 30].

2.3.1. UHI intensity

UHI intensity $\Delta T_{(urban\text{-}rural)}$ measures the difference between air temperature of an urban area and its surrounding rural area. Average hourly temperature readings at MK, CWB and HKO were plotted and compared against TYW readings to determine their respective UHI intensities over a 24 hour period. Both summer and winter data were plotted alongside for contrast and comparison.

The urban and rural temperature results were contrasted based on the diurnal temperature range (DTR). DTR is the difference between the daily maximum temperature and minimum temperature and has been found to be inversely proportional to the level of urbanization [31, 32, 33]. Pearson’s r correlation and Student's t-test were employed to examine the seasonal association between urban and rural DTR.

2.3.2. Statistical analysis of meteorological and environmental factors

Meteorological conditions have been known to have ameliorating or amplifying effects on the UHI [34]. In this research, the local meteorological parameters available by portable weather station measurements included air temperature, relative humidity, solar radiation, rainfall, peak wind speed, wind speed, and wind directions. Each of the aforementioned meteorological factors were entered or removed from automatic linear regression modeling at p=0.05 statistical significance [35, 36]. The regression models were evaluated using four selection criteria: Akaike information criterion corrected (AICC), F- statistics, adjusted R-squared, and average squared error (ASE). All outputs of ranks and coefficients were compared and contrasted to indicate the order of importance of meteorological factors and their corresponding influential effects on local UHI intensity at MK and CWB.

Urban morphology and other urban environmental variables are known to influence the levels of UHI [37, 38]. In this study, a number of environmental (annual average daily traffic - AADT, building density, greenery density, road density, topography, and sky view factor - SVF) and socio-economic (social deprivation index – SDI[2], population density and household density) variables were tested using statistical regression analysis to establish their seasonal association with UHI in urban areas (MK and CWB combined). All of the aforementioned variables at MK and CWB were spatially determined by a 100m circular buffer around each of the site measurement locations. A smaller buffer size (100m) was used for local scale effect studies [39, 40]. All predictor variables were entered or removed from the automatic linear regression model in a forward stepwise manner at p=0.05 statistical significance [35, 36, 41]. The AICC, F-statistics, adjusted R-squared, and ASE were used to evaluate the regression models.

2.3.3. Analysis of temperature variation in different environmental settings

Microclimate temperature variations were computed for five environmental settings (main road, secondary road, public activity, park and tunnel) across MK and CWB. Each of the five local temperature measurements across MK and CWB were illustrated by box plot graphs. Official urban (HKO) and rural (TYW) temperatures were also referenced.

It is known that cooling rates in rural areas are greater than urban areas [17, 42] and the differences of cooling rates between urban and rural areas will influence the diurnal cycle of UHI effects [34]. The 24-hour cooling rate is mathematically defined as the rate of air temperature change per hour. To further evaluate the five categories of environmental settings, their respective 24-hour cooling rates for summer and winter were computed by averaging all representative hourly temperature data in each setting. The respective maximum cooling rates at each setting were summarized for comparison. Finally, Pearson's r correlation and Student's t-test were employed to examine the statistical and seasonal difference in cooling rates for each type of environmental settings.

3. Results

Field measurements of sensors were validated to establish data reliability and accuracy of the device. Sensor readings were consistently higher (0.26 ºC higher on average) compared to official measurements at the HKO. The root mean square error was 0.31 ºC indicating that the average difference of sensor measurements was well within the ±1 ºC accuracy (±0.5 ºC with software correction) as claimed by the manufacturer.

3.1. Temporal variation of UHI

Figures 5a and 5b display the 24-hour summer and winter average hourly temperature plots respectively for four locations in Hong Kong (MK, CWB, HKO, and TYW). MK and CWB averages were computed using measurements from all surveyed locations (containing a variation of microclimates of different environmental settings) whereas HKO and TYW were measurements from the respective official weather stations. All three urban settings (MK, CWB and HKO) exhibited similar patterns of fluctuation in the temperature measurements for both seasons. The two study sites (MK and CWB) experienced warmer summer and winter temperatures than similar measurements at the HKO. This observation is expected because the sensors were positioned in bustling neighborhoods of MK and CWB whereas the official HKO site was situated in a park. Summer temperature measurements at the TYW were comparatively cooler than its urban counterparts except between 0830 and 1530 during which a reversed trend was observed only between HKO and TYW (Figure 5a). This reversal of temperature difference (at 0.54 °C on average) is known as the urban cool island (UCI) effect [43] whilst nighttime temperatures at the HKO were 2-3 °C warmer. A similar reversal trend of 0.43 °C in winter temperature difference was observed only between HKO and TYW for the period between 0930 and 1600 (about 1-hour time delay compared to the summer observation; Figure 5b).

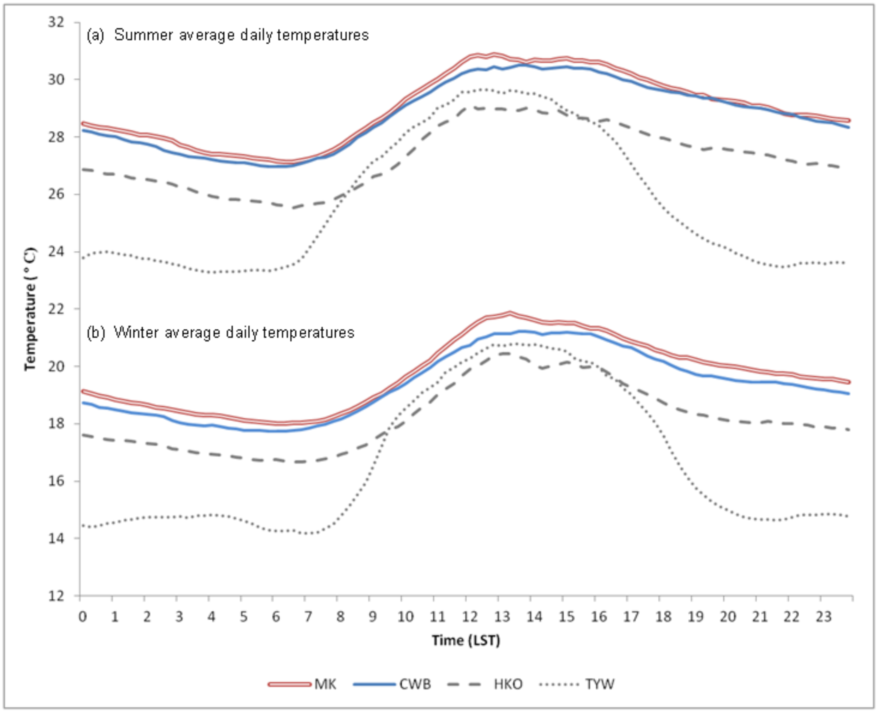

Figure 5: (a) Summer and (b) winter average daily temperature measurements at various locations in Hong Kong. Mong Kok (MK – red double line) and Causeway Bay (CWB – blue solid line) are urban communities. Hong Kong Observatory (HKO - dashed line) and Tsak Yue Wu (TYW - dotted line) represent official urban and rural weather stations respectively. Note that readings from the two urban communities were always higher than those of official stations.

Table 1 summarizes the average diurnal temperature range (DTR) in both seasons for all locations differentiated by urban and rural settings. Although temperatures in cities tended to be warmer than those in outlying rural areas, urbanized areas often show a narrower DTR [32]. Our observations and statistical results confirmed significant urban-rural temperature differences and the presence of UHI in MK and CWB over the temporal scale.

Table 1: A statistical summary of diurnal temperature range (DTR) between urban and rural locations

Season	**Summer**		**Winter**	
Site	Urban (MK, CWB, HKO)	Rural (TYW)	Urban (MK, CWB, HKO)	Rural (TYW)
DTR	3.53	6.37	3.70	6.61
Pearson's r	0.81*		0.90*	
Means Test	0.00*		0.00*	

* Statistical significance at p=0.05

3.2. Meteorological Factors influencing UHI

Table 2 displays the outcomes of automatic linear regression models based on two study locations and two seasons. Four different model criteria (AICC or Akaike's Information Criterion Corrected, F-Statistics, Adjusted R-square, and ASE or Average Squared Error) were used to evaluate the rankings and coefficients of different variables in their respective criteria for two different seasons in MK and CWB. The smaller the information criterion values of the models, the better the model fits in the regression [44].

Table 2: A summary of ranks and coefficients of meteorological variables in linear regression models.

	Season	Model Criteria	Information Criterion	Wind Speed	Peak Wind Speed	Rainfall	Solar Radiation	Temperature	Relative Humidity	Wind Direction	Intercept
UHI_{MK}	Summer	AICC	-32.317	4(-1.147)	-	-	**1(-0.029)**	2(-1.032)	3(-0.198)	-	46.723
		F-Statistics	-32.317	4(-1.147)	-	-	**1(-0.029)**	2(-1.032)	3(-0.198)	-	46.723
		Adjusted R	-32.121	-	-	-	**1(-0.028)**	2(-0.978)	3(-0.200)	-	45.603
		ASE	-28.852	-	-	-	**1(-0.029)**	2(-0.974)	3(-0.200)	-	45.392
	Winter	AICC	8.939	-	3(-1.150)	-	**1(-0.010)**	-	2(-0.118)	-	13.911
		F-Statistics	8.939	-	3(-1.150)	-	**1(-0.010)**	-	2(-0.118)	-	13.911
		Adjusted R	8.939	-	3(-1.150)	-	**1(-0.010)**	-	2(-0.118)	-	13.911
		ASE	15.872	-	-	-	**1(-0.011)**	-	-	-	17.734
UHI_{CWB}	Summer	AICC	-32.595	-	-	-	3(-0.028)	2(-2.226)	**1(-0.281)**	4(-0.003)	83.651
		F-Statistics	-32.595	-	-	-	3(-0.028)	2(-2.226)	**1(-0.281)**	4(-0.003)	83.651
		Adjusted R	-32.595	-	-	-	3(-0.028)	2(-2.226)	**1(-0.281)**	4(-0.003)	83.651
		ASE	-31.203	-	-	-	3(-0.027)	2(-2.115)	**1(-0.275)**	4(-0.004)	80.585
	Winter	AICC	-18.508	3(2.763)	-	-	**1(-0.017)**	-	-	2(0.004)	1.359
		F-Statistics	-17.765	3(1.739)	-	-	**1(-0.018)**	-	-	2(0.004)	1.038
		Adjusted R	-24.911	5(2.330)	-	-	**1(-0.017)**	3(-1.135)	4(-0.285)	2(0.005)	44.621
		ASE	-24.911	5(2.330)	-	-	**1(-0.017)**	3(-1.135)	4(-0.285)	2(0.005)	44.621

Note: Seven meteorological factors were included in the regression analysis for UHI_{MK} and UHI_{CWB} in both seasons. These variables included wind speed, peak wind speed, rainfall, solar radiation, temperature, relative humidity, and wind direction. The number besides the left bracket indicates rank of that variable in the regression model. "1" means the first variable ranked in the stepwise regression model and "4" means the fourth. The number within the brackets indicates the coefficient of that variable in the regression model. A positive or negative sign shows the type of relationships. Only significant variables ($p< 0.05$) are shown in the table. Boldfaced text highlights most important or first ranked variable.

AICC = Akaike's information criterion corrected; ASE = Average squared error.

The top half of Table 2 shows that solar radiation consistently appeared as the most important contributing or ranked 1 factor of the UHI in MK (UHI_{MK}) based on all four criterion measures. It was also clear that solar radiation had a negative correlation with UHI in both seasons, meaning that the UHI would be weakened as the solar radiation increased. When solar radiation increases, rural areas with less shading will be exposed to direct sunlight, thus narrowing the thermal difference between urban and rural areas. Table 2 also shows that the ranked 2 variable of UHI_{MK} was temperature in the summer and relative humidity in the winter. Both independent variables had a negative correlation with UHI_{MK} suggesting that warmer temperatures would weaken summer UHI_{MK} while higher levels of relative humidity would weaken winter UHI_{MK}.

The bottom half of Table 2 shows slightly different results for UHI_{CWB}. Relative humidity replaced solar radiation to be the ranked 1 variable, followed by temperature in the second place for summer UHI_{CWB}. All predictor variables had a negative correlation with summer UHI_{CWB}, meaning that a higher value for relative humidity, temperature and solar radiation would weaken summer UHI_{CWB}. Solar radiation remained as the most important predictor that had a negative correlation with winter UHI_{cwb}. However, the ranked 2 and positively correlated variable of wind direction suggested that a larger angle away from 0 °N would increase winter UHI_{cwb}. In other words, the Victoria Harbor to the north of CWB favored northerly winds in the winter time to advect warm air at the street levels which, in turn, minimized the thermal contrast between urban and rural areas.

3.3. Environmental Factors influencing UHI

Table 3 shows the statistical outcomes of automatic linear regression models between the dependent variable (UHI_{MK} and UHI_{CWB} combined) and various environmental and socio-economic variables over two seasons. Although the rankings and coefficients of importance variables influencing UHI_{Summer} and UHI_{Winter} were similar, the AICCs with the smallest information criterion values (-92.276 and -100.780 for summer and winter respectively) were recognized as the best fit regression models. The AICC regression model results in Table 3 confirmed the importance of greenery in reducing UHI in both seasons. It is also obvious from Table 3 that social deprivation index (SDI) had a significant association with the UHI but only in the summer. The positive association indicates that socially deprived households tended to reside in areas with higher UHI. Similarly, the positive association of topography with UHI in the winter indicates that a lower ground elevation is associated with a smaller UHI value and vice versa. Other variables tested did not show consistent or significant association with the UHI.

Table 3: A summary of ranks and coefficients of environmental and socio-economic variables in linear regression models.

	Model Summary		Environmental						Socio-economic			
	Model Criteria	Information Criterion	AADT	Building Density	Greenery Density	Road Density	Topography	SVF	SDI	Population Density	Household Density	Intercept
Summer	**AICC**	**-92,276**	**-**	**-**	**1(-0.062)**	**-**	**-**	**-**	**2(0.238)**	**-**	**-**	**2.126**
	F-Statistics	-90.858	2(0.000)	-	3(-0.041)	-	-	-	1(0.329)	-	-	0.299
	Adjusted R	-92.204	-	-	1(-0.062)	-	-	-	-	-	-	2.517
	ASE	-89,589	-	2(-0.025)	1(-0.062)	-	-	-	-	-	-	3.064
Winter	**AICC**	**-100.780**	**-**	**-**	**1(-0.014)**	**-**	**2(0.050)**	**-**	**-**	**-**	**-**	**4.358**
	F-Statistics	-100.258	-	-	1(-0.015)	-	2(0.052)	-	-	-	-	4.462
	Adjusted R	-100.305	-	-	1(-0.013)	-	2(0.050)	-	-	-	-	4.317
	ASE	-94.832	-	-	1(-0.017)	-	-	-	-	-	-	4.589

Note: The number within the brackets indicates the coefficient of that variable in the regression model. A positive or negative sign shows the type of relationships. Only significant variables ($p < 0.05$) are shown in the table.

AADT = Annual average daily traffic; SDI = Social deprivation index; SVF = Sky view factor
AICC = Akaike's information criterion corrected; ASE = Average squared error

Five different environmental settings were examined for possible causes of temperature variability. Figure 6 shows that the average summer and winter temperature measurements for all environmental settings in MK and CWB were above the average official urban (HKO) measurements (black horizontal lines). The categories of "main road" and "public activity" among other settings appeared to record comparatively warmer temperatures in both seasons. "Tunnel", being semi-enclosed and without direct solar radiation, appeared to experience lesser variation in temperatures although they were still fairly warm compared to the official urban setting at HKO. The cooling effects of greeneries were more obvious in CWB than MK in the winter season because "park" in CWB is larger in size, has more trees and lesser artificial surfaces.

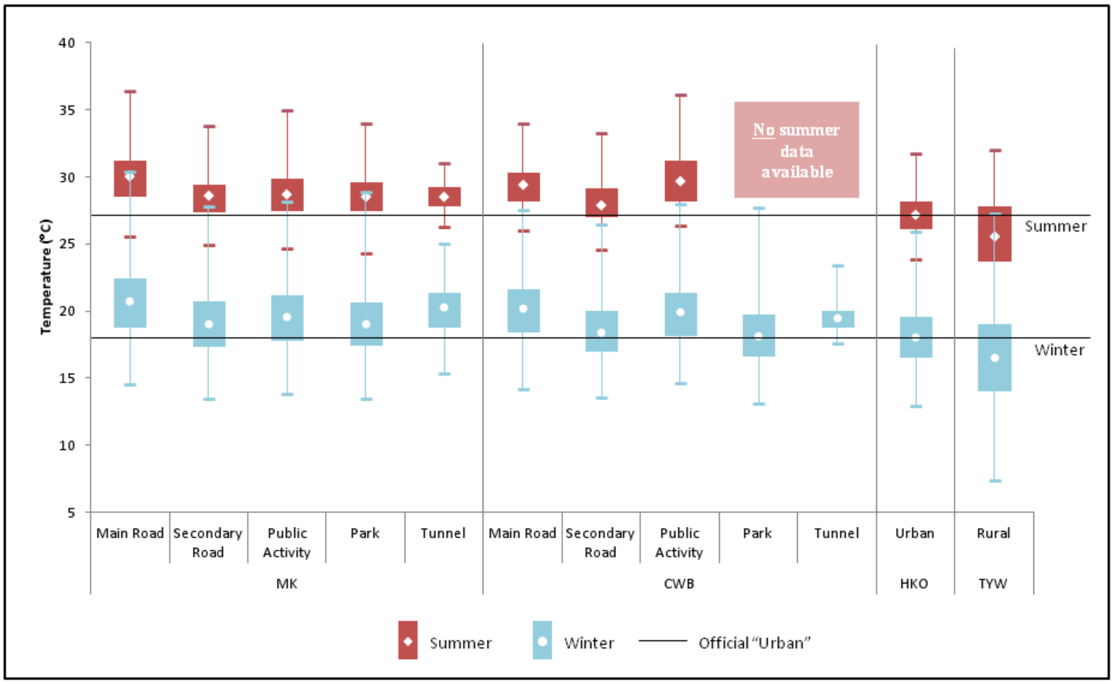

Figure 6: Boxplots of sensor measurements by specific environmental settings in Mong Kok (MK) and Causeway Bay (CWB). Summer temperatures are shown in red boxplots (with a hollow diamond in the middle) and winter temperatures in blue boxplots (with a hollow circle in the middle). Boxplots of the official urban (HKO) and rural (TYW) measurements are shown on the rightmost end. (Note: Sensors were missing for summer measurements in the park and tunnel at CWB.)

To further evaluate the five different environmental settings, their representative temperature data were used to determine the respective diurnal cooling rates. The 24-hour cooling rates in both seasons demonstrated similar trends comparable to those of the official urban location at HKO. The 24-hour cooling rates (referencing the maximum rate of change of air temperature per setting) and their statistical outcomes at each environmental setting in MK and CWB are summarized in Table 4. TYW in the rural area registered the highest 24-hour cooling rate compared to all the other urban locations. The Pearson's correlation coefficients revealed a relatively strong correlation ($r > 0.69$) between the summer and winter cooling rates at each of the environmental settings in MK and CWB. The Student's t-test for each of the urban settings denoted no significant seasonal differences ($p > 0.98$).

Table 4: A statistical summary of 24-hour cooling rate across five environment settings in Mong Kok (MK) and Causeway Bay (CWB): main road, secondary road, public activity, park, and tunnel. The official urban (HKO) and rural (TYW) measurements are shown on the right.

Cooling rates in °C/h	MK					CWB					HKO	TYW
	Main Road	Secondary Road	Public Activity	Park	Tunnel	Main Road	Secondary Road	Public Activity	Park	Tunnel	HKO	TYW
Summer	0.48	0.57	0.84	0.42	0.32	0.55	0.53	0.87	-	-	0.37	1.48
Winter	0.75	0.69	0.58	0.80	0.45	0.64	0.62	0.57	0.97	0.12	0.69	1.81
Pearson's r	0.69*	0.84*	0.85*	0.82*	0.76*	0.79*	0.83*	0.73*	-	-	0.64*	0.83*
Means test	0.99	0.99	0.99	1.00	1.00	0.99	0.99	0.98	-	-	1.00	1.00

* Statistical significance at p=0.05

4. Discussion

Time-series sensor data collected in MK and CWB for summer and winter provided empirical evidence about the temporal behavior of UHI. The average daily DTR between urban (MK, CWB and HKO) and rural (TYW) settings revealed strong and statistically significant seasonal correlation ($r>0.81$, $p=0.00$ in Table 1). Temporal variation of UHI was evident for all time scales, with daily highest UHI at around midnight and daily lowest at around noon to early afternoon which exhibited urban cool island (UCI) effects. The one-hour time lag in winter UHI was due to delayed sunrise. Overall, the official summer and winter UHI_{HKO} during the study period ranged between 0 and 2 °C but both UHI_{MK} and UHI_{CWB} ranged between 2 and 4 °C. This difference in UHI intensities in urbanized areas with a high level of human activity and heavy transportation (i.e., MK and CWB in Figure 6) signified a more severe UHI problem requiring further examination.

The formation of UHI and the identification of its controlling or casual factors in an urban setting involve a complex process. The automatic linear regression analysis yielded dissimilar results about UHI intensities in MK and CWB for different seasons. Different meteorological and environmental variables seemed to exert varying degrees of influence on the UHIs depending on the location and the season. The statistical identification of factors influencing UHI has benefited microclimate UHI studies in urban areas of Hong Kong. Apart from re-confirming the mitigating effect of greenery on UHIs in both seasons, the study also identified solar radiation to be a major factor influencing UHIs. The small coefficient values of greenery compared with other research findings [45, 46] could be a result of the low density and patchy arrangement of pocket parks in MK that reduced its positive impact on UHIs. The findings of solar radiations coupled with observed UCI effects in urban areas during midday suggested the prevalence of shading effects from built structures over strong wind advection at the street level.

This study also found significant microclimate variations (a difference of 2 °C) within the urban and densely populated areas of different environmental settings. Areas categorized as "main road" and "public activity" appeared to record comparatively warmer temperatures for both seasons. The presence of built structures and artificial surfaces from urbanization affected the diurnal cooling rates due to higher thermal conductivities and capacities of urban surfaces. The concentration of anthropogenic activities from transportation and crowding has a major role in contributing to urban heat.

5. Conclusion

Empirical evidence about microclimate UHI variation in districts with different meteorological and environmental settings has enriched the comparative understanding of UHI in urban communities of Hong Kong. The findings show that microclimate variation does exist within an urban area as a result of the interplay between urban morphology and local meteorological factors. Although temporal behavior of daily UHI was found to follow the theoretical pattern, spatial variability of microclimate involved complex interactions and very much location dependent. This study also empirically suggested the degree of heat impact is more severe in areas of high public activity and heavy transportation despite the fact that Hong Kong is known for its compact urban forms with highly efficient and convenient transportation. An understanding of microclimate variations will benefit policy management to pay more attention to the UHI problem in urban design. Specifically, further research on examining the greenery effects of pocket parks with limited vegetation in urban areas of Hong Kong is needed to inform best practice in urban design pursuing compact urban development.

This microclimate UHI study was made possible through flexible deployment of logging sensors in the two most densely populated areas of Hong Kong, namely MK and CWB. The study filled research and data gaps on microclimate studies in urban areas of subtropical climate. Instead of simulating warming effects on local environmental conditions, the inexpensive and reliable temperature sensors increase the ability not only to record microclimatic conditions but also to explore many questions pertaining to the problems of urban heat. This microclimate study is exemplary in terms of the integrated use of case study and GIS approach that provides empirical evidence and theoretical implications of the temporal and location specific behavior of the UHI phenomenon. It aids the further understanding on local issues of human comfort and brings in the broader picture of environmental health in an urban setting.

Footnotes

1 The Mass Transit Railway (MTR) is a light rail network and is the most convenient and a major means of public transportation in Hong Kong. The MTR exits are known as one of core locations of high human activity that collectively delimit the extent where population gathers for social and economic engagement.

2 The social deprivation index (SDI) is the average of the proportions of population in six census variables: a) unemployment, b) monthly household income < US$250, c) no schooling at all, d) one-person household, e) never-married status, and f) subtenancy [47]. The range of SDI is between 0 and 100 with larger SDI values implying that residents in the corresponding census areas endure greater disadvantages and lower socioeconomic status.

Acknowledgement

This research was funded partially by the Hong Kong Research Grants Council (HKU 744113) and the University of Hong Kong Graduate School. Acknowledgement is also due to Fulbright and Lee Hysan Foundation. The Authors would like to thank the following government departments for granting permissions to install sensors on street signs for continuous roadside measurement: Department of Transport, Highways Department, and Leisure and Cultural Services Department of the Hong Kong SAR. Thanks are also extended to Hong Kong Observatory (HKO) for providing access to specific weather stations to calibrate and validate sensors.

References

[1] Gabriel, K. M. A. & Endlicher, W. R. (2011) Urban and rural mortality rates during heat waves in Berlin and Brandenburg, Germany. *Environmental Pollution*, 159 (8-9), 2044-2050.

[2] Kleerekoper, L., van Esch, M. & Salcedo, T. B. (2012) How to make a city climate-proof, addressing the urban heat island effect. *Resources, Conservation and Recycling*, 64 (0), 30-38.

[3] Akbari, H., Davis, S., Dorsano, S., Huang, Y. J. & Winnett, S. (1992) *Cooling Our Communities: A Guidebook on Tree Planting and Light-Colored Surfacing*. United States Environmental Protection Agency.

[4] Roth, M. (2007) Review of urban climate research in (sub)tropical regions. *International Journal of Climatology*, 27 (14), 1859-1873.

[5] Singh, R. B. (2014) *Urban Development Challenges, Risks and Resilience in Asian Mega Cities*. Springer Japan.

[6] Angotti, T., Beckel, L. & Agency, E. S. (2001) *Mega Cities: The European Space Agency's Contribution to a Better Understanding of a Global Challenge*. GEOSPACE.

[7] Giridharan, R., Lau, S. S. Y., Ganesan, S. & Givoni, B. (2008) Lowering the outdoor temperature in high-rise high-density residential developments of coastal Hong Kong: The vegetation influence. Building and Environment, 43 (10), 1583-1595.

[8] Dimoudi, A., Kantzioura, A., Zoras, S., Pallas, C. & Kosmopoulos, P. (2013) Investigation of urban microclimate parameters in an urban center. *Energy and Buildings*, 64 (0), 1-9.

[9] Taleghani, M., Tenpierik, M., van den Dobbelsteen, A. & Sailor, D. J. (2014) Heat mitigation strategies in winter and summer: Field measurements in temperate climates. *Building and Environment*, 81, 309-319.

[10] Met Office (2011) Microclimates. *The National Meteorological Library and Archive - Fact sheet 14.* UK, Met Office.

[11] Lau, S. S., Lin, P. & Qin, H. (2012) A preliminary study on environmental performances of pocket parks in high-rise and high-density urban context in Hong Kong. *International Journal of Low-Carbon Technologies*, 7 (3), 215-225.

[12] Wong, N. H. & Chen, Y. (2009) *Tropical urban heat islands : climate, buildings and greenery*. Taylor & Francis. 259 pp.

[13] Mirzaei, P. A. (2015) Recent challenges in modeling of urban heat island. *Sustainable Cities and Society*.

[14] Priyadarsini, R., Hien, W. N. & Wai David, C. K. (2008) Microclimatic modeling of the urban thermal environment of Singapore to mitigate urban heat island. *Solar Energy*, 82 (8), 727-745.

[15] Tominaga, Y. (2012) Visualization of city breathability based on CFD technique: case study for urban blocks in Niigata City. *Journal of Visualization*, 15 (3), 269-276.

[16] Planning Department. (2014) *Land Utilization in Hong Kong*. [Online]. Available from: http://www.pland.gov.hk/pland_en/info_serv/statistic/landu.html [Accessed 2014].

[17] Siu, L. & Hart, M. (2013) Quantifying urban heat island intensity in Hong Kong SAR, China. *Environmental Monitoring and Assessment*, 1-16.

[18] Ingham, M. (2007) *Hong Kong: A Cultural and Literary History*. Signal Books.
[19] Stewart, I. D. & Oke, T. R. (2012) Local Climate Zones for Urban Temperature Studies. *Bulletin of the American Meteorological Society*, 93 (12), 1879-1900.
[20] LCSD. (2013) *Victoria Park - The Leisure and Cultural Service Department of HKSAR*. [Online]. Available from: http://www.lcsd.gov.hk/parks/vp/en/index.php [Accessed June, 2013].
[21] Planning Department. (2005) *Shopping Survey*. [Online]. Available from: http://www.pland.gov.hk/pland_en/p_study/comp_s/shopping/e_index.htm [Accessed July 2013].
[22] Shaker, R. R. & Drezner, T. D. (2010) A New Technique for Predicting the Sky-View Factor for Urban Heat Island Assessment. *The Geographical Bulletin*, 51, 85-96.
[23] Hjort, J., Suomi, J. & Käyhkö, J. (2011) Spatial prediction of urban–rural temperatures using statistical methods. Theoretical and Applied Climatology, 106 (1-2), 139-152.
[24] Arnfield, A. J. (2003) Two decades of urban climate research: a review of turbulence, exchanges of energy and water, and the urban heat island. *International Journal of Climatology*, 23 (1), 1-26.
[25] Bagienski, Z. (2015) Traffic air quality index. *The Science of the total environment*, 505, 606-14.
[26] World Meteorological Organization (2008) *Guide to Meteorological Instruments and Methods of Observation (Seventh edition)*. World Meteorological Organization. WMO-No.8.
[27] Hong Kong Observatory. (2013) *The Hong Kong Observatory Official Website*. [Online]. Available from: http://www.hko.gov.hk/contente.htm [Accessed Jan 2013].
[28] Maxim (2009) *DS1923 iButton Capsule Data Sheet*. Maxim Integrated Products. 19-4991; Rev 3;.
[29] Fung, W. Y., Lam, K. S., Nichol, J. & Wong, M. S. (2009) Derivation of Nighttime Urban Air Temperatures Using a Satellite Thermal Image. *Journal of Applied Meteorology and Climatology*, 48 (4), 863-872.
[30] Oke, T. (1988) The urban energy balance. *Progress in Physical Geography*, 12 (4), 471-508.
[31] Price, C., Michaelides, S., Pashiardis, S. & Alpert, P. (1999) Long term changes in diurnal temperature range in Cyprus. *Atmospheric Research*, 51 (2), 85-98.
[32] Wang, K., Ye, H., Chen, F., Xiong, Y. & Wang, C. (2011) Urbanization Effect on the Diurnal Temperature Range: Different Roles under Solar Dimming and Brightening*. *Journal of Climate*, 25 (3), 1022-1027.
[33] Shahid, S., Harun, S. B. & Katimon, A. (2012) Changes in diurnal temperature range in Bangladesh during the time period 1961–2008. *Atmospheric Research*, 118 (0), 260-270.
[34] Oke, T. R. (1982) The energetic basis of the urban heat island. *Quarterly Journal of the Royal Meteorological Society*, 108 (455), 1-24.
[35] Miller, A. (2002) *Subset Selection in Regression (2nd Edition)*. Taylor & Francis.
[36] Bottyán, Z. & Unger, J. (2003) A multiple linear statistical model for estimating the mean maximum urban heat island. *Theoretical and Applied Climatology*, 75 (3-4), 233-243.
[37] Upmanis, H., Eliasson, I. & Lindqvist, S. (1998) The influence of green areas on

nocturnal temperatures in a high latitude city (Göteborg, Sweden). *International Journal of Climatology*, 18 (6), 681-700.

[38] Unger, J. (2006) Modelling of the annual mean maximum urban heat island using 2D and 3D surface parameters. *Climate Research*, 30 (3), 215-226.

[39] Oke, T. R. (1987) *Boundary Layer Climates*. Methuen, U.S.A, Routledge.

[40] Nichol, J. E. & Wong, M. S. (2008) Spatial variability of air temperature and appropriate resolution for satellite derived air temperature estimation,. *International Journal of Remote Sensing*, 29 (24), 7213-7223.

[41] Field, A. (2013) *Discovering Statistics using IBM SPSS Statistics*. SAGE Publications.

[42] Makokha, G. L. & Shisanya, C. A. (2010) Temperature Cooling and Warming Rates in Three Different Built Environments within Nairobi City, Kenya. *Advances in Meteorology*, 2010.

[43] Memon, R., Leung, D., Liu, C.-H. & Leung, M. (2011) Urban heat island and its effect on the cooling and heating demands in urban and suburban areas of Hong Kong. *Theoretical and Applied Climatology*, 103 (3), 441-450.

[44] IBM.com. (2012) *SPSS Statistics v.20 manual: case studies on linear models*. [Online]. Available from: http://pic.dhe.ibm.com/infocenter/spssstat/v20r0m0/index.jsp?topic=%2Fcom.ibm.spss.statistics.cs%2Flinear_insurance_howto.htm [Accessed Oct, 2013].

[45] Saito, I., Ishihara, O. & Katayama, T. (1990) Study of the effect of green areas on the thermal environment in an urban area. *Energy and Buildings*, 15 (3–4), 493-498.

[46] Ng, E., Chen, L., Wang, Y. & Yuan, C. (2012) A study on the cooling effects of greening in a high-density city: An experience from Hong Kong. *Building and Environment*, 47 (0), 256-271.

[47] Wong, C. M., Ou, C. Q., Chan, K. P., Chau, Y. K., Thach, T. Q., Yang, L., Chung, R. Y., Thomas, G. N., Peiris, J. S. M. & Wong, T. W. (2008) The effects of air pollution on mortality in socially deprived urban areas in Hong Kong, China. *Environmental Health*, 116 (9), 1189-1194.

Table captions

1 A statistical summary of diurnal temperature range (DTR) between urban and rural locations.

2 A summary of ranks and coefficients of meteorological variables in linear regression models.

3 A summary of ranks and coefficients of environmental and socio-economic variables in linear regression models.

4 A statistical summary of 24-hour cooling rate across five environment settings in Mong Kok (MK) and Causeway Bay (CWB): main road, secondary road, public activity, park, and tunnel. The official urban (HKO) and rural (TYW) measurements are shown on the right.

Figure captions

1 A map of Hong Kong showing locations of Mong Kok (MK) and Causeway Bay (CWB). The Hong Kong Observatory (HKO) and Tsak Yue Wu (TYW) are the designated urban and rural weather stations respectively.

2 Mong Kok and Causeway Bay with radial buffers of 200m and 400m based on MTR exits.

3 Set up of a monitoring sensor.

4 The maps show locations of sensors and local controls in (a) Mong Kok and (b) Causeway Bay. Five different environmental settings were surveyed: main road, secondary road, public activity, park and tunnel. Figure shows photographs of street scenes and corresponding fish eye images at the respective survey sites in Mong Kok and Causeway Bay.

5 (a) Summer and (b) winter average daily temperature measurements at various

locations in Hong Kong. Mong Kok (MK – red double line) and Causeway Bay (CWB – blue solid line) are urban communities. Hong Kong Observatory (HKO - dashed line) and Tsak Yue Wu (TYW - dotted line) represent official urban and rural weather stations respectively. Note that readings from the two urban communities were always higher than those of official stations.

6 Boxplots of sensor measurements by specific environmental settings in Mong Kok (MK) and Causeway Bay (CWB). Summer temperatures are shown in red boxplot (with diamond in the middle) and winter temperatures in blue boxplot (with circle in the middle). Boxplots of the official urban (HKO) and rural (TYW) measurements are shown on the right. (Note: sensors for summer measurements in the park and tunnel at CWB were missing.)